

Gravitational Lensing by Burkert Halos

Yousin Park^{1,2} and Henry C. Ferguson^{2,1}

ypark@stsci.edu, ferguson@stsci.edu

ABSTRACT

We investigate the gravitational lensing properties of dark matter halos with Burkert profiles. We derive an analytic expression for the lens equation and use it to compute the magnification, impact parameter and image separations for strong lensing. For the scaling relation that provides the best fits to spiral-galaxy rotation curve data, Burkert halos will not produce strong lensing, even if this scaling relation extends up to masses of galaxy clusters. Tests of a simple model of an exponential stellar disk superimposed on a Burkert-profile halo demonstrate that strong lensing is unlikely without an additional concentration of mass in the galaxy center (e.g. a bulge). The fact that most strong lenses on galactic scales are elliptical galaxies suggests that a strong central concentration of baryons is required to produce image splitting. This solution is less attractive for clusters of galaxies, which are generally considered to be dark-matter dominated even at small radii. There are three possible implications of these results: (1) dark halos may have a variety of inner profiles (2) dark matter halos may not follow a single scaling relation from galaxy scale up to cluster scale and/or (3) the splitting of images (even by clusters of galaxies) may in general be due to the central concentration of baryonic material in halos rather than dark matter.

Subject headings: gravitational lensing — galaxies: halo

1. Introduction

It is currently believed that structure in the universe formed with nearly scale-free initial conditions from quantum fluctuations during the early parts of the inflationary phase. Subsequent growth of structure depends in part on the nature of the dark matter (DM);

¹Department of Physics and Astronomy, The Johns Hopkins University, Baltimore, MD 21218

²Space Telescope Science Institute, Baltimore, MD 21218

specifically if it is cold (non-relativistic at the epoch of matter–radiation decoupling), as would be the case for axions, clustering proceeds hierarchically with small structures collapsing before large ones. The exact nature of this evolution depends on the cosmological parameters and the nature of the DM. If the DM is entirely collisionless and cold, halos are expected to form with a nearly universal profile, independent of the final mass of the halo. A specific functional form for this profile was proposed by Navarro, Frenk & White (1996, hereafter NFW) on the basis of N-body simulations of hierarchical structure formation.

On a galaxy/sub-galaxy scale, the NFW profile for DM halos has been severely challenged by observations of rotation curves of disk galaxies (e.g. de Blok et al. 2001; Borriello & Salucci 2001). The rotation curves of low-surface-brightness (LSB), low-mass galaxies tend to rise significantly more slowly with radius than the NFW prediction. The Burkert profile for DM halos was proposed to explain the rotation curves of four dwarf galaxies (Burkert 1995), and appears to provide an excellent mass model for DM halos around disk systems up to 100 times more massive (Salucci & Burkert 2000). For the DM halos harboring elliptical galaxies, Keeton (2001) shows that the NFW profile is too concentrated to explain observed gravitational lensing. Recently, Borriello, Salucci & Danese (2002) show that the NFW profile is inconsistent with the Fundamental Plane (FP), and that the FP can be successfully explained with the Burkert profile. On a cluster scale, Wu & Xue (2000) find that the Burkert and NFW profiles provide almost indistinguishable fits to ROSAT cluster X-ray data. All this evidence suggests that the Burkert profile is a *plausible* candidate for the DM halos on both galaxy and cluster scales, though it was empirically proposed and its physical origin is less well understood than the NFW profile.

Gravitational lensing offers a promising way to distinguish the different proposed halo profiles. In this letter we present an analytical expression for the Burkert-profile lens equation and show that this profile will produce strong lensing only for a certain combination of concentration index and lens–source distances. We find that Burkert halos of any mass are unlikely to act as strong lenses unless the spiral-galaxy scaling relation between characteristic mass and density breaks down on larger mass scales, or other (e.g. baryonic) components of the object provide the cusp necessary for image splitting.

In § 2, we present the lens equation for the Burkert profile. In § 3, we explore the properties of the Burkert lens and examine the implications of these properties. In § 4, we summarize and discuss the results. In this letter, we consider Λ CDM model: $\Omega_M = 0.3$ and $\Omega_\Lambda = 0.7$ with a Hubble constant $H_0 = 100h\text{km/s/Mpc}$ and $h = 0.75$.

2. Lens Equation for the Burkert Profile

The Burkert profile has a constant density core (Burkert 1995):

$$\rho(r) = \frac{\rho_s}{(1 + r/r_s)[1 + (r/r_s)^2]}, \quad (1)$$

where ρ_s and r_s are free parameters that represent the central DM density and the scale radius. The NFW profile has singularity at its center:

$$\rho_{\text{NFW}}(r) = \frac{\rho_s}{r/r_s(1 + r/r_s)^2}. \quad (2)$$

At very large radii, two profiles coincide: $\rho \sim r^{-3}$.

In the thin lens approximation, the lens equation for an axially symmetric mass profile is essentially one dimensional:

$$\psi(\theta) = \theta - \frac{D_{LS}}{D_S} \frac{4GM_p(D_L|\theta|)}{c^2 D_L \theta}, \quad (3)$$

where $D_{LS} = D_A(z_L, z_S)$, $D_L = D_A(0, z_L)$ and $D_S = D_A(0, z_S)$. Here, z_L and z_S are respectively the redshifts of the lens and the source, and $D_A(z_1, z_2)$ is the angular-diameter distance from z_1 to z_2 . And, ψ and θ are respectively the positions of the source ($\psi \geq 0$) and the image, and $M_p(\xi)$ is the projected mass enclosed within a projected radius ξ :

$$M_p(\xi) = 2\pi \int_0^\xi x dx \int_{-\infty}^\infty dz \rho(\sqrt{x^2 + z^2}) = 4\pi \rho_s r_s^3 a\left(\frac{\xi}{r_s}\right). \quad (4)$$

The function $a(x)$ can be worked out analytically:

$$a(x) = \begin{cases} \ln \frac{x}{2} + \frac{\pi}{4}(\sqrt{x^2 + 1} - 1) + \frac{\sqrt{x^2 + 1}}{2} \operatorname{arccoth} \sqrt{x^2 + 1} - \frac{1}{2} \sqrt{x^2 - 1} \arctan \sqrt{x^2 - 1} & (x > 1) \\ -\ln 2 - \frac{\pi}{4} + \frac{1}{2\sqrt{2}}[\pi + \ln(3 + 2\sqrt{2})] & (x = 1) \\ \ln \frac{x}{2} + \frac{\pi}{4}(\sqrt{x^2 + 1} - 1) + \frac{\sqrt{x^2 + 1}}{2} \operatorname{arccoth} \sqrt{x^2 + 1} + \frac{1}{2} \sqrt{1 - x^2} \operatorname{arctan} h\sqrt{1 - x^2} & (x < 1). \end{cases} \quad (5)$$

The equivalent factor for the NFW profile, $a_{\text{NFW}}(x)$, is given by Bartelmann (1996).

With $\beta \equiv D_L \psi / r_s$, $\alpha \equiv D_L \theta / r_s$, one can write the dimensionless lens equation:

$$\beta(\alpha) = \alpha - \lambda \frac{a(|\alpha|)}{\alpha} \quad (6)$$

with

$$\lambda = 16\pi \frac{G \rho_s r_s}{c^2} \frac{D_L D_{LS}}{D_S} = 7.21 h^{-1} \left(\frac{\rho_s}{M_\odot \text{pc}^{-3}} \right) \left(\frac{r_s}{\text{kpc}} \right) \frac{d_L d_{LS}}{d_S}, \quad (7)$$

where the reduced angular-diameter distance d_A is defined to be $d_A \equiv D_A H_0 / c$. In this letter, we use the angular diameter distance of the Friedmann-Robertson-Walker universe.

3. Lensing Properties and Implications

The parameter λ determines all the properties of the Burkert-profile lens. Fig. 1 shows the lens equations for different values of λ . For $0 < \lambda \leq \lambda_c = 8/\pi$, Burkert halos cannot induce strong lensing. In contrast, the NFW halos can induce strong lensing for any λ . Fig. 2 shows magnification μ of the Burkert halos for different values of λ : $\mu = d\alpha^2/d\beta^2$. For $\lambda = 4 > \lambda_c$, two peaks in the magnification curve correspond to the radial and tangential arcs respectively. For $\lambda \leq \lambda_c$, the magnification curves have the peak at $\alpha = 0$.

Modeling strong lensing with the Burkert halos requires $\lambda > \lambda_c$, for which multiple images are formed only if the impact parameter $\beta \leq \beta_c$. Here, β_c is the maximum of $\beta(\alpha)$ in the range $\alpha < 0$ (see Fig. 1). The cross section for strong lensing by the Burkert halos is $\sigma = \pi(\beta_c r_s / D_L)^2$. If $\beta = 0$, then an Einstein ring is formed at the radius α_t , which is a positive solution of $\alpha_t^2 = \lambda a(\alpha_t)$. (For a lens at $z_L = 0.5$ with a scale radius $r_s = 30\text{kpc}$, $\alpha_t = 0.1$ corresponds to $\Delta\theta \approx 1''$.) For $0 < \beta < \beta_c$, three images are formed. The separation between the two brighter images is $\Delta\theta \approx 2\alpha_t r_s / D_L$. Fig. 3 shows the critical impact parameter β_c and the Einstein radius α_t as a function of λ for the Burkert and NFW halos. While the impact parameter of the Burkert halo is always less than that of the NFW halo for fixed λ , the image separation α_t of the Burkert halos becomes larger than that of the NFW halos when λ becomes greater than ≈ 7 .

The difference between the two profiles near $r = 0$ leads to a dramatic difference in the cross section for strong lensing for a given image separation $\Delta\theta$ or α_t . For small separations (say, $\alpha_t \lesssim 0.1$) the impact parameter β_c required for the Burkert halo to induce splitting is considerably smaller than that of the NFW halo. For example, the ratios are 8.9×10^{-4} and 3.2×10^{-2} for $\alpha_t = 0.01, 0.1$ respectively; the relative cross sections scale as β_c^2 . Thus for the same distribution of r_s , the lensing optical depth due to Burkert halos is almost vanishingly small compared to that due to NFW halos. This is particularly true for lensing by galaxy-scale objects; for example the probability for a QSO image to be split by a single intervening giant elliptical galaxy is at least 10^3 times smaller for a Burkert profile than for an NFW profile, for the same r_s and mass. This is not true for large image separations ($\alpha_t \gtrsim 1$) as might be the case for giant arcs formed by cluster-scale lenses. In this case the Burkert halos yield optical depths comparable to the NFW halos, though slightly less (by a factor ~ 0.1 to 0.5).

The condition $\lambda > \lambda_c$ corresponds to restricted area in the (ρ_s, r_s) parameter plane. The condition can be rephrased as:

$$\left(\frac{\rho_s}{\text{M}_\odot \text{pc}^{-3}}\right) \left(\frac{r_s}{\text{kpc}}\right) > f(z_L, z_S) \quad (8)$$

where

$$f(z_L, z_S) = 0.353h \frac{d_S}{d_L d_{LS}}. \quad (9)$$

In Fig. 4 we plot strong lensing demarcation curves: $(\rho_s/M_\odot \text{pc}^{-3})(r_s/\text{kpc}) = f_m(z_S)$ for $z_S = 1, 3, 5$. Here, $f_m(z_S)$ is the minimum of $f(z_L, z_S)$ in the range $0 < z_L < z_S$. Burkert halos with (ρ_s, r_s) located above the demarcation curve for a given z_S can induce strong lensing, those below the demarcation curve cannot.

The rotation curves of late-type LSB galaxies and dwarfs suggest that Burkert halos for these galaxies lie in a narrow strip in the (ρ_s, r_s) plane: $\rho_s/M_\odot \text{pc}^{-3} = 4.5 \times 10^{-2}(r_s/\text{kpc})^{-2/3}$, which is the thick solid line in Fig. 4. Salucci & Burkert (2000) confirmed the relation for disk galaxies up to 100 times more massive. At the highest masses in their sample there is an apparent change of slope, suggesting a cutoff in the masses of halos that harbor individual disk galaxies at $M \sim 2 \times 10^{12} M_\odot$.

We overplot some of these low-redshift measurements in Fig. 4. The black circles with error bars are from the recent H α rotation curves of late-type dwarf galaxies by Marchesini et al. (2002), which lie near the scaling relation line. For comparison, we add the lensing cluster CL0024+1654 at $z_L = 0.39$. The central density and scale radius of the cluster are estimated by Firmani et al. (2001). Though the cluster is claimed to have soft core (Tyson, Kochanski & Dell’Antonio 1998; however see Broadhurst et al. 2000), there is no evidence that the cluster has the Burkert profile. The cluster is clearly well off the scaling relation defined by low-redshift disk galaxies (which, like the cluster, are argued to be dark-matter dominated over most of their observed radii).

It is clear that the mass profiles of strong strong lens systems (e.g. Kochanek et al. 2003) must be cuspier than the Burkert profiles on the spiral-galaxy scaling relation. If these systems have Burkert profile DM halos, then the baryonic matter in these systems must be distributed in a much steeper way than the DM. It is then the baryonic matter (not DM) that induces strong lensing. Unless the baryonic matter has very steep core profiles, the total mass profile will remain close to the Burkert profile and still be highly unlikely to induce strong lensing. For example, the inclusion of exponential stellar disk effectively reduces the λ_c for face-on spirals:

$$\lambda_c = \frac{8}{\pi + 2\Sigma_0/\rho_s r_s}, \quad (10)$$

where Σ_0 is the surface density of the stellar disk at $\xi = 0$. For an L^* spiral with $M_{\text{disk}} = 2 \times 10^{11} M_\odot$, we obtain $\Sigma_0 \approx 702 M_\odot \text{pc}^{-2}$, the disk scale length $r_d \approx 4.76 \text{kpc}$, $\rho_s \approx 3.78 \times 10^{-3} M_\odot \text{pc}^{-3}$ and $r_s \approx 19.3 \text{kpc}$ from the relation of Salucci & Borriello (2002), who extend the scaling relation of Burkert halos including the exponential stellar disk. For this system (the

rotational velocity $v_c = 240\text{km/s}$ at $r = 10\text{kpc}$), we have $\lambda_c \approx 0.357$, which is significantly less than $8/\pi$. However, λ is less than 0.18 up to $z_S = 8$, which means that the face-on L^* spiral systems (Burkert halo + exponential stellar disk) cannot produce strong lensing up to $z_S = 8$, unless other baryonic matter such as a bulge is included.

Fig. 4 also shows that the Burkert halos extrapolated from the late-type galaxy scaling relation cannot be used to account for lensing on cluster scales ($r_s \gtrsim 100\text{kpc}$). One can model a lensing cluster with a Burkert halo, whose (ρ_s, r_s) should be beyond the demarcation line for a given z_S as those of the galaxy cluster CL0024+1654 are. The cluster can induce strong lensing for $z_S > 1.0$, not for $z_S < 1.0$ if the cluster is indeed a Burkert halo. If DM halos at cluster scales do have the Burkert profile, there must be (at least) two different families of the Burkert halos.

4. Discussion

We present an analytic lens equation for the Burkert halos, and use it to characterize their lensing properties. We show that, as a result of their soft core, the Burkert halos are much less likely to induce strong lensing than the NFW halos. While the qualitative result is fairly obvious, when calculated in detail, the differences in the strong-lensing predictions for the two profiles turn out to be quite dramatic. If galaxies are indeed harbored by the Burkert halos, it implies that the baryonic matter (not DM) is responsible for strong lensing and that it is distributed in a much steeper way than the Burkert profile in strong lensing systems. For strong lensing systems (mostly elliptical galaxies), the total mass profiles for these systems have steeper inner slopes than the Burkert profile (Koopmans & Treu 2003). It remains to be seen whether this is due to a distribution of baryons or cusps in the DM profile for these systems.

On a galaxy scale, lens modeling combining stellar and DM components has been carried out for the NFW profile (e.g. Keeton 2001) and is proving to be a useful tool to test the validity of the proposed DM profile. Similar modeling with the Burkert profile will test its validity. On a cluster scale, the validity of the Burkert halos can be tested through galaxy kinematics (e.g. Sand, Treu & Ellis 2002) and X-ray observations (e.g. Wu & Xue 2000). The detailed test methods will be addressed in future articles. While challenging, it also may be feasible to constrain halo profiles by combining measurements of tangential shear and strong lensing for the same objects.

We are grateful to Stefano Casertano for numerous conversations, sage advice, and insightful comments on the manuscript. Support for this work was provided by the Director's

Discretionary Research Fund at the Space Telescope Science Institute, which is operated by AURA, Inc., under NASA contract NAS 5-26555.

REFERENCES

- Bartelmann, M. 1996, *A&A*, 313, 697
- Borriello, A. & Salucci, P. 2001, *MNRAS*, 323, 285
- Borriello, A., Salucci, P. & Danese, L. 2002, astro-ph/0208268
- Broadhurst, T., Huang, X., Frye, B. & Ellis, R. 2000, *ApJ*, 534, L15
- Bullock, J. S., Kolatt, T. S., Sigad, Y., Somerville, R. S., Kravtsov, A. V., Klypin, A. A., Primack, J. R. & Dekel, A. 2001, *MNRAS*, 321, 559
- Burkert, A. 1995, *ApJ*, 447, L25
- de Blok, W. J. G., McGaugh, S. S., Bosma, A. & Rubin, V. C. 2001, *ApJ*, 552, L23
- Firmani, C., D’Onghia, E., Chincarini, G., Hernández, X. & Avila-Reese, V. 2001, *MNRAS*, 321, 713
- Keeton, C. R. 2001, *ApJ*, 561, 46
- Kochanek, C. S., Falco, E. E., Impey, C. D., Lehár, J., McLeod, B. A. & Rix, H.-W. 2003, CfA/Arizona Space Telescope Lens Survey website <http://cfa-www.harvard.edu/castles>
- Koopmans, L. V. E. & Treu, T. 2003, *ApJ*, 583, 606
- Marchesini, D., D’Onghia, E., Chincarini, G., Firmani, C., Conconi, P., Molinari, E. & Zacchei, A. 2002, *ApJ*, 575, 801
- Navarro, J. F., Frenk, C. S. & White, S. D. M. 1996, *ApJ*, 462, 563
- Salucci, P. & Boriello, A. 2002, astro-ph/0203457
- Salucci, P. & Burkert, A. 2000, *ApJ*, 537, L9
- Sand, D. J., Treu, T. & Ellis, R. S., 2002, *ApJ*, 574, L129
- Tyson, J. A., Kochanski, G. P. & Dell’Antonio, I. P. 1998, *ApJ*, 498, L107
- Wu, X. & Xue, Y. 2000, *ApJ*, 542, 578

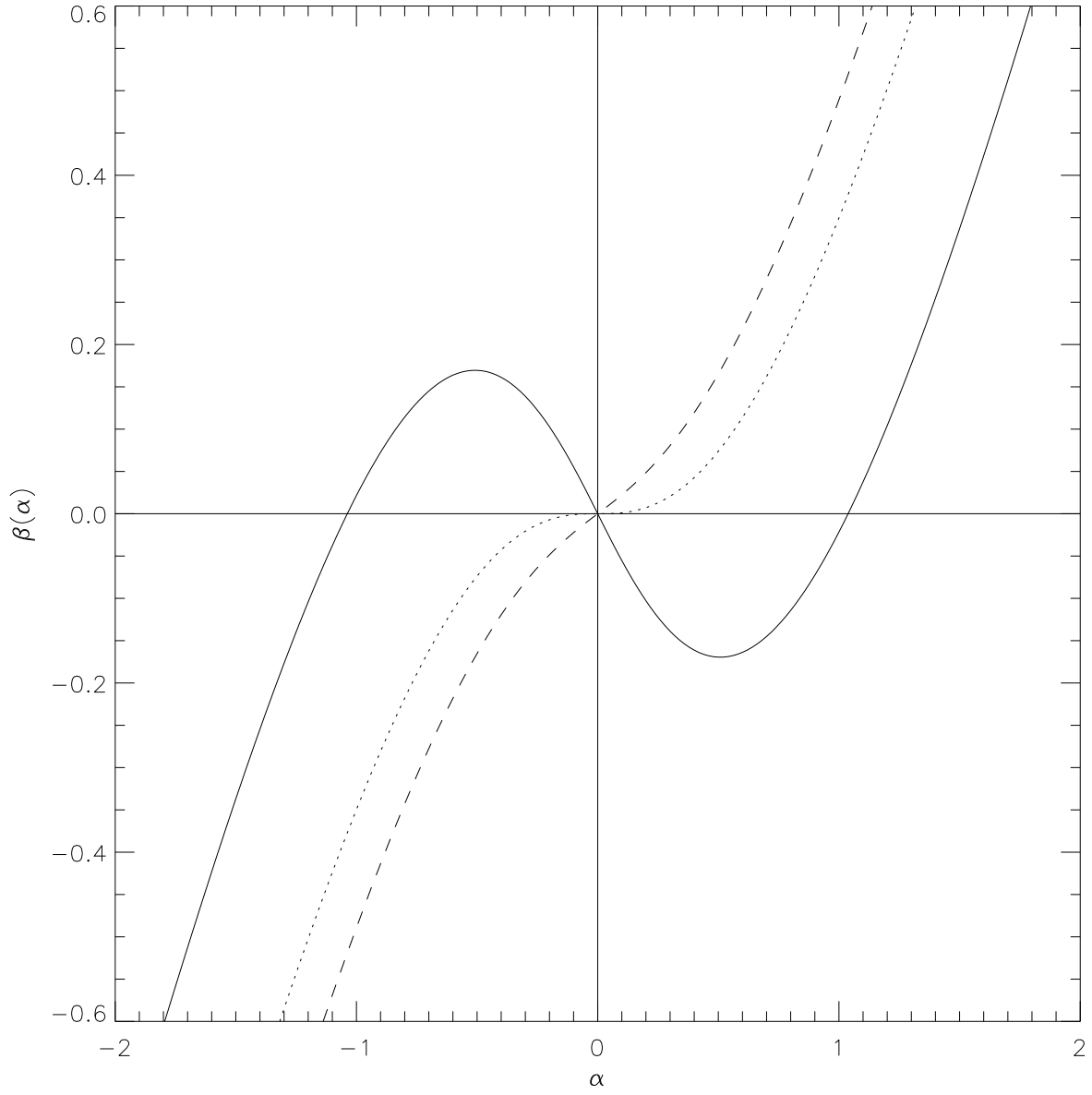


Fig. 1.— Lens equation for the Burkert profile. The solid, dotted and dashed lines are respectively for $\lambda = 4, 8/\pi, 2$. Only lens–source combinations with $\lambda > 8/\pi$ will produce multiple images.

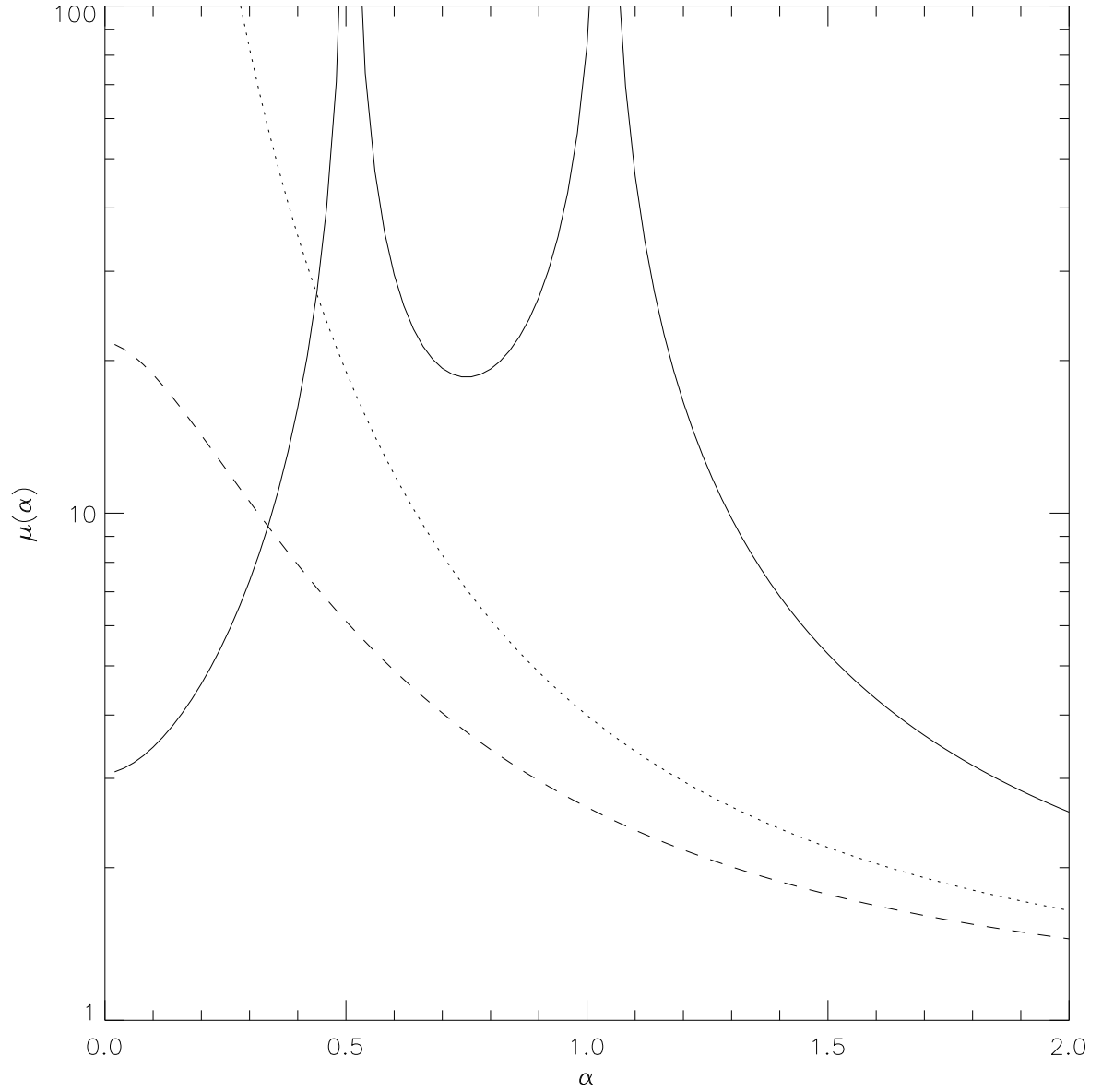


Fig. 2.— Magnification as a function of image position for the Burkert profile. The solid, dotted and dashed lines are respectively for $\lambda = 4, 8/\pi, 2$. The inner and outer peaks in the magnification function for $\lambda = 4$ are for radial and tangential arcs, respectively.

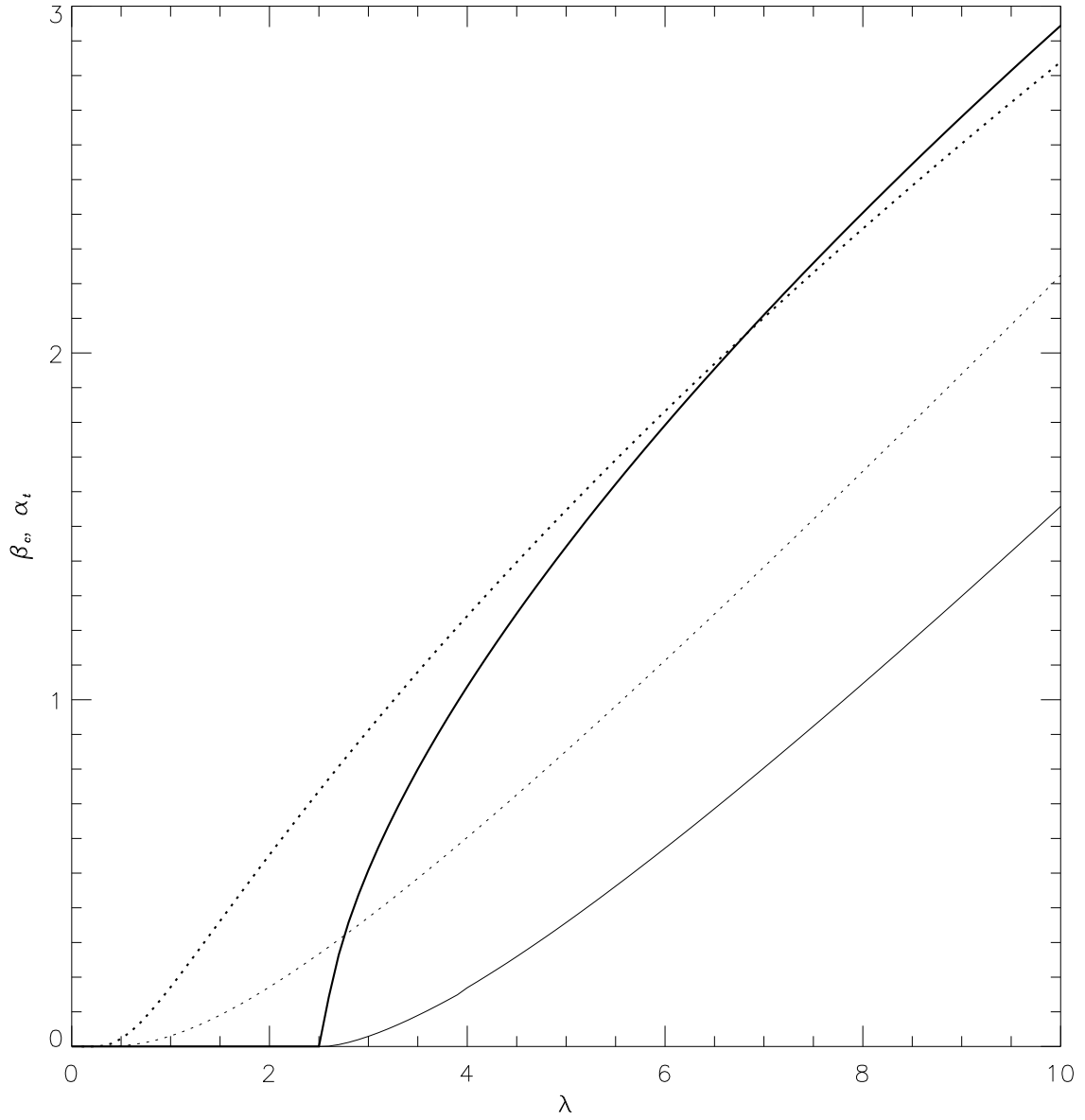


Fig. 3.— The impact parameter β_c (thin lines) and image separation α_t (thick lines) as a function of λ for the Burkert and NFW profiles. The solid and dotted curves are for the Burkert and NFW profiles, respectively.

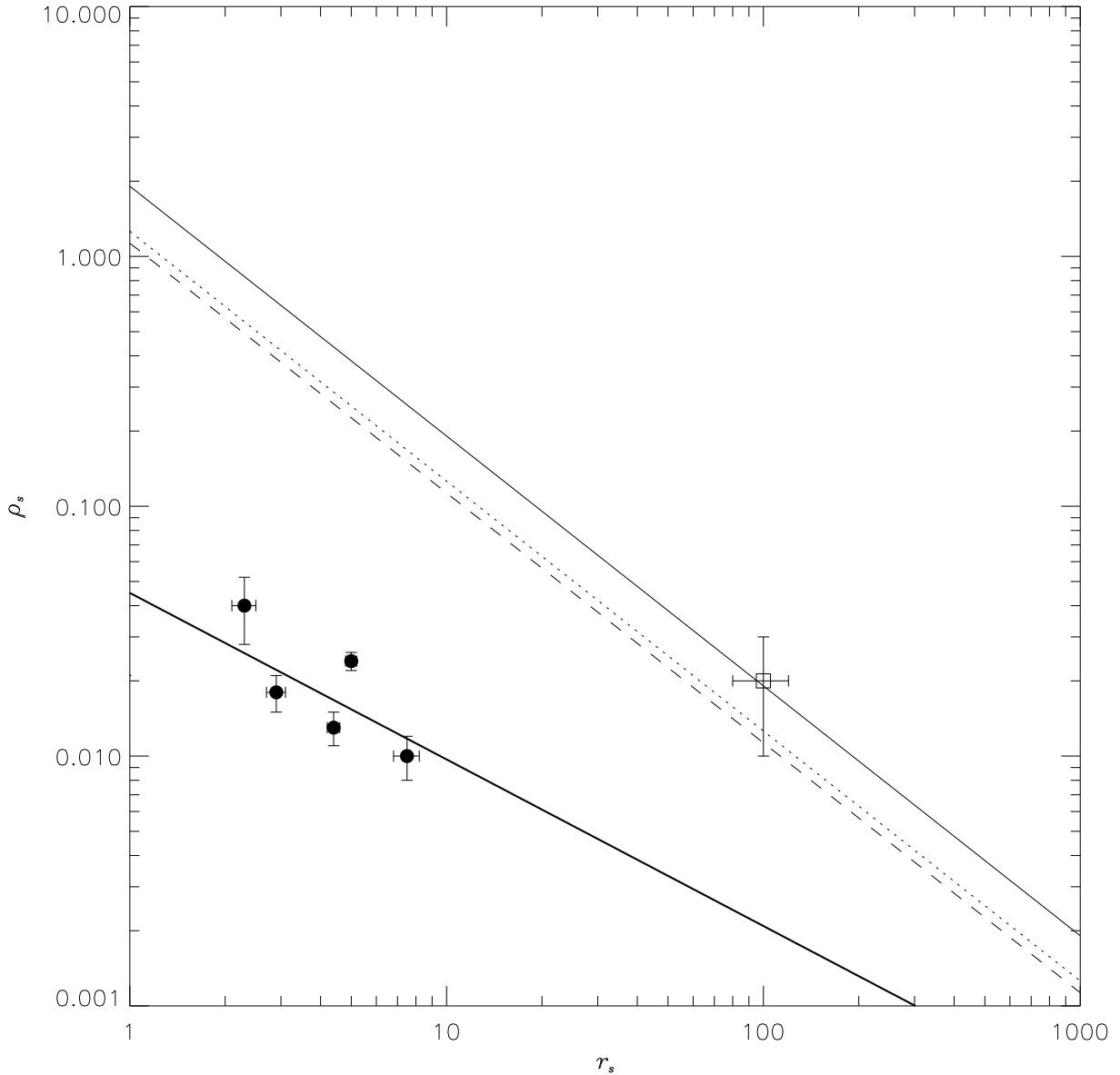


Fig. 4.— Strong lensing demarcation curves for $z_S = 1, 3, 5$. The thin solid, dotted and dashed lines are respectively for source redshifts $z_S = 1, 3, 5$. The thick solid line is the scaling relation of the Burkert halos at $z \approx 0$. The black circles with error bars are from rotation-curve measurements of late-type low-surface-brightness galaxies and dwarfs (Marchesini et al. 2002). The square represents the halo parameters for the lensing cluster CL0024+1654 estimated by Firmani et al. (2001). The units of ρ_s and r_s are $M_\odot \text{pc}^{-3}$, kpc respectively.